



**HAL**  
open science

## **HEATR3 variants impair nuclear import of uL18 (RPL5) and drive Diamond-Blackfan anemia**

Marie-Françoise O'Donohue, Lydie da Costa, Marco Lezzerini, Sule Unal, Clément Joret, Marije Bartels, Eva Brilstra, Marijn Scheijde-Vermeulen, Ludivine Wacheul, Kim de Keersmaecker, et al.

► **To cite this version:**

Marie-Françoise O'Donohue, Lydie da Costa, Marco Lezzerini, Sule Unal, Clément Joret, et al.. HEATR3 variants impair nuclear import of uL18 (RPL5) and drive Diamond-Blackfan anemia. *Blood*, 2022, 10.1182/blood.2021011846 . hal-03664461

**HAL Id: hal-03664461**

**<https://hal.science/hal-03664461>**

Submitted on 10 Oct 2023

**HAL** is a multi-disciplinary open access archive for the deposit and dissemination of scientific research documents, whether they are published or not. The documents may come from teaching and research institutions in France or abroad, or from public or private research centers.

L'archive ouverte pluridisciplinaire **HAL**, est destinée au dépôt et à la diffusion de documents scientifiques de niveau recherche, publiés ou non, émanant des établissements d'enseignement et de recherche français ou étrangers, des laboratoires publics ou privés.



American Society of Hematology  
 2021 L Street NW, Suite 900,  
 Washington, DC 20036  
 Phone: 202-776-0544 | Fax 202-776-0545  
 editorial@hematology.org

## **HEATR3 variants impair nuclear import of uL18 (RPL5) and drive Diamond-Blackfan anemia**

Tracking no: BLD-2021-011846R3

Marie-Françoise O'Donohue (Université de Toulouse, France) Lydie Da Costa (Laboratory of Excellence for Red Cells, France) Marco Lezzerini (Amsterdam UMC, Netherlands) Sule Unal (Research Center of Fanconi Anemia and Other Inherited Bone Marrow Failure Syndromes, Turkey) Clément Joret (Université Libre de Bruxelles, Belgium) Marije Bartels (University Medical Center, Netherlands) Eva Brilstra (University Medical Center Utrecht, Netherlands) Marijn Scheijde-Vermeulen (Princess Máxima Center for Pediatric Oncology, Netherlands) Ludivine Wacheul (Université libre de Bruxelles, Belgium) Kim De Keersmaecker (KU Leuven, Belgium) Stijn Vereecke (KU Leuven, Belgium) Veerle Labarque (University Hospitals Leuven, Belgium) Manon Saby (Inserm, France) SOPHIE LEFEVRE (UNIVERSITE DE PARIS, France) Jessica Platon (UPJV, France) Nathalie Montel-Lehry (Université de Toulouse, France) Nathalie Laugero (Inserm/UPS UMR 1297 - I2MC, France) Eric Lacazette (UMR 1297-I2MC INSERM, France) Riekelt Houtkooper (Amsterdam UMC, Netherlands) Pelin Ozlem Simsek-Kiper (Hacettepe University, Turkey) Thierry Leblanc (Hôpital Robert-Debré - Assistance Publique-Hôpitaux de Paris, France) Nese Yarali (Yıldırım Beyazıt University Ankara City Hospital Children's Hospital, Turkey) Arda Cetinkaya (Hacettepe University, Turkey) Nurten Akarsu (Hacettepe University, Turkey) Pierre-Emmanuel Gleizes (Université de Toulouse, France) Denis Lafontaine (Université libre de Bruxelles, Belgium) Alyson MacInnes (Amsterdam UMC, Netherlands)

### **Abstract:**

The congenital bone marrow failure syndrome, Diamond-Blackfan anemia (DBA), is typically associated with variants in ribosomal protein (RP) genes impairing erythroid cell development. Here we report multiple individuals with biallelic *HEATR3* variants exhibiting bone marrow failure, short stature, facial and acromelic dysmorphic features, and intellectual disability. These variants destabilize a protein whose yeast homolog is known to synchronize the nuclear import of ribosomal proteins uL5 (RPL11) and uL18 (RPL5), which are both critical for producing ribosomal subunits and for stabilizing the p53 tumor suppressor when ribosome biogenesis is compromised. Primary cells, cell lines of various origins, and yeast models with *HEATR3* variants or reductions reveal defects in growth, differentiation, pre-rRNA processing, and ribosomal subunit formation reminiscent of DBA models of large subunit RP gene variants. Consistent with a role of *HEATR3* in RP import, cells with *HEATR3* variants or knockdowns reveal reduced nuclear accumulation of uL18. Hematopoietic progenitor cells with *HEATR3* variants or reductions reveal abnormal acceleration of erythrocyte maturation coupled to severe proliferation defects that are independent of p53 activation. Our study uncovers a new pathophysiological mechanism leading to DBA driven by biallelic *HEATR3* variants and the destabilization of a nuclear import protein important for ribosome biogenesis.

**Conflict of interest:** No COI declared

**COI notes:**

**Preprint server:** No;

**Author contributions and disclosures:** Involved in the clinical care and molecular diagnosis of the individuals in the study: S.U., P.O.S.K., N.Y., A.C., N.A.A., L.D.C., M.B., E.B., K.V.G., M.S.V., K.D.K., S.V., V.L., T.L. Designed the study: A.M.W., M.O.D., L.D.C., M.B., P.E.G., D.L.J.L. Designed and performed experiments: M.O.D., M.L., C.J., M.S., S.L., L.W., N.L., E.L., N.M.L., J.P. Analyzed and interpreted data: A.M.W., M.O.D., L.D.C., M.L., C.J., R.H.H., P.E.G., D.L.J.L. Contributed to the preparation and critical reviewing of manuscript: S.U., A.C., N.A.A., M.O.D., L.D.C., M.B., K.D.K., V.L., P.E.G., D.L.J.L. Drafted the manuscript: A.M.W. Revised the manuscript: A.M.W., P.E.G., D.L.J.L.

**Non-author contributions and disclosures:** No;

**Agreement to Share Publication-Related Data and Data Sharing Statement:** Disease-causing HEATR3 variants have been submitted to ClinVar. Data supporting the findings of this study are available upon request by e-mails to the corresponding authors.

**Clinical trial registration information (if any):**

# **HEATR3 variants impair nuclear import of uL18 (RPL5) and drive Diamond-Blackfan anemia**

**Running title:** HEATR3 variants drive Diamond-Blackfan anemia

Marie-Françoise O'Donohue<sup>1\*</sup>, Lydie Da Costa<sup>2,3,4,5\*</sup>, Marco Lezzerini<sup>6\*</sup>, Sule Unal<sup>7,8\*</sup>, Clément Joret<sup>9</sup>, Marije Bartels<sup>10</sup>, Eva Brilstra<sup>11</sup>, Marijn Scheijde-Vermeulen<sup>12</sup>, Ludivine Wacheul<sup>9</sup>, Kim De Keersmaecker<sup>13</sup>, Stijn Vereecke<sup>13</sup>, Veerle Labarque<sup>14</sup>, Manon Saby<sup>15</sup>, Sophie D. Lefevre<sup>4,15</sup>, Jessica Platon<sup>3</sup>, Nathalie Montel-Lehry<sup>1</sup>, Nathalie Laugero<sup>16</sup>, Eric Lacazette<sup>16</sup>, Koen van Gassen<sup>11</sup>, Riekelt H. Houtkooper<sup>6</sup>, Pelin Ozlem Simsek-Kiper<sup>17</sup>, Thierry Leblanc<sup>18</sup>, Nese Yarali<sup>19</sup>, Arda Cetinkaya<sup>20</sup>, Nurten A. Akarsu<sup>20</sup>, Pierre-Emmanuel Gleizes<sup>1§</sup>, Denis L.J. Lafontaine<sup>9§</sup>, Alyson W. MacInnes<sup>6</sup>

Abstract word count: 198

Main Text (Intro, M&M, Results, Discussion) word count: 3975

Figure/Table count: 7 Figures / 2 Tables

Reference count: 51

---

<sup>1</sup> MCD, Centre de Biologie Intégrative, Université de Toulouse, CNRS, UT3, 31000 Toulouse, France.

<sup>2</sup> University of Paris, F-75010, Paris, France.

<sup>3</sup> Hematim EA4666, UPJV, F-80000, Amiens, France.

<sup>4</sup> Laboratory of Excellence for Red Cells, LABEX GR-Ex, F-75015, Paris, France.

<sup>5</sup> Service d'Hématologie Biologique, AP-HP, Hôpital Robert Debré, F75019, Paris, France.

<sup>6</sup> Amsterdam UMC, University of Amsterdam, Laboratory Genetic Metabolic Diseases, Amsterdam Gastroenterology, Endocrinology, and Metabolism, Meibergdreef 9, 1105 AZ Amsterdam, The Netherlands.

<sup>7</sup> Hacettepe University, Medical Faculty, Department of Pediatrics, Pediatric Hematology Unit, 06230, Ankara, Turkey.

<sup>8</sup> Hacettepe University, Research Center of Fanconi Anemia and Other Inherited Bone Marrow Failure Syndromes, 06230, Ankara, Turkey.

<sup>9</sup> RNA Molecular Biology, Fonds de la Recherche Scientifique (F.R.S./FNRS), Université libre de Bruxelles (ULB), Biopark campus, B-6041 Gosselies, Belgium.

<sup>10</sup> University Medical Center Utrecht, Department of Pediatric Hematology, 3508 AB Utrecht, The Netherlands.

<sup>11</sup> University Medical Center Utrecht, Department of Genetics, 3508 AB Utrecht, The Netherlands.

<sup>12</sup> Princess Máxima Center for Pediatric Oncology, Department of Pathology, 3584 CS Utrecht, the Netherlands

<sup>13</sup> Laboratory for Disease Mechanisms in Cancer, Department of Oncology, KU Leuven and Leuven Cancer Institute (LKI), Herestraat 49, 3000 Leuven, Belgium.

<sup>14</sup> University Hospitals Leuven, Department of Pediatric Hemato-Oncology, Herestraat 49, 3000 Leuven, Belgium.

<sup>15</sup> Inserm UMR S1134, F-75015, Paris, France.

<sup>16</sup> UMR 1297-I2MC, Inserm, Université de Toulouse, UT3, 31432 Toulouse cedex 4, France.

<sup>17</sup> Hacettepe University, Medical Faculty, Department of Pediatrics, Pediatric Genetics Unit, 06230, Ankara, Turkey.

<sup>18</sup> Immuno-Hematology Department, Hôpital Robert-Debré, Assistance Publique-Hôpitaux de Paris, 75019 Paris, France and EA-3518, Université Paris-Diderot, Paris, France

<sup>19</sup> Yildirim Beyazit University, Medical Faculty, Department of Pediatrics, Pediatric Hematology Unit, 06010 Ankara, Turkey.

<sup>20</sup> Hacettepe University, Medical Faculty, Department of Medical Genetics, 06230, Ankara, Turkey.

\* Equal contribution

§Corresponding authors: [pierre-emmanuel.gleizes@univ-tlse3.fr](mailto:pierre-emmanuel.gleizes@univ-tlse3.fr) (+33 561 55 83 00) and [denis.lafontaine@ulb.be](mailto:denis.lafontaine@ulb.be) (+32 473 97 39 62)

## KEY POINTS

- Biallelic variants in *HEATR3* are associated with DBA and other clinical features in humans
- *HEATR3* variants destabilize the protein, resulting in a reduction of nuclear uL18 and impaired ribosome biogenesis

## ABSTRACT

The congenital bone marrow failure syndrome, Diamond-Blackfan anemia (DBA), is typically associated with variants in ribosomal protein (RP) genes impairing erythroid cell development. Here we report multiple individuals with biallelic *HEATR3* variants exhibiting bone marrow failure, short stature, facial and acromelic dysmorphic features, and intellectual disability. These variants destabilize a protein whose yeast homolog is known to synchronize the nuclear import of ribosomal proteins uL5 (RPL11) and uL18 (RPL5), which are both critical for producing ribosomal subunits and for stabilizing the p53 tumor suppressor when ribosome biogenesis is compromised. Expression of *HEATR3* variants or repression of *HEATR3* expression in primary cells, cell lines of various origins, and yeast models impairs growth, differentiation, pre-rRNA processing, and ribosomal subunit formation reminiscent of DBA models of large subunit RP gene variants. Consistent with a role of *HEATR3* in RP import, *HEATR3*-depleted cells or patient-derived fibroblasts display reduced nuclear accumulation of uL18. Hematopoietic progenitor cells expressing *HEATR3* variants or small-hairpin RNAs knocking down *HEATR3* synthesis reveal abnormal acceleration of erythrocyte maturation coupled to severe proliferation defects that are independent of p53 activation. Our study uncovers a new pathophysiological mechanism leading to DBA driven by biallelic *HEATR3* variants and the destabilization of a nuclear import protein important for ribosome biogenesis.

## INTRODUCTION

Ribosomopathies are rare human disorders resulting from impaired production of ribosomes. Many variants in different ribosomal protein (RP) genes drive Diamond-Blackfan anemia (DBA). Rare cases were also associated with the transcription factor *GATA1* and the ribosomal assembly factor *TSR2*, while DBA-like syndromes were linked to variants of the genes encoding the adenosine deaminase *ADA2* or the serum protein *EPO*.<sup>1-4</sup> DBA is characterized by a paucity of erythroid progenitor and precursor cells in the bone marrow and red cell aplasia that is frequently (~50%) associated with physical malformations of the face, hands (abnormal thumbs), heart, and urogenital tract.<sup>5</sup> Individuals with DBA also have an increased risk of developing cancer, including AML and osteosarcomas.<sup>6</sup> Inherited RP gene mutations have been reported in individuals with asplenia, intellectual disability (ID), autism, and/or dysmorphism but no hematological phenotype.<sup>7-11</sup> Suggested mechanisms underlying DBA include stabilization of the p53 tumor suppressor, the reduced translation of transcripts important for erythropoiesis such as *GATA1*, *BAG1*, and *CSDE1*, and/or the degradation of the *GATA1* chaperone *HSP70*.<sup>1,12-17</sup>

*RPL5* and *RPL11* encode uL18 and uL5, respectively, which uniquely assemble in the nucleus with 5S rRNA to form the 5S RNP, a complex that incorporates with maturing large ribosomal subunits to form the central protuberance.<sup>18</sup> When ribosome biogenesis is compromised and the 5S RNP is not incorporated, it accumulates in free form and associates with Hdm2. This interaction inhibits the Hdm2 ubiquitin ligase function that normally targets p53 for constitutive proteasomal degradation.<sup>19</sup> This anti-tumor regulatory loop, known as 'nucleolar surveillance', regulates the p53 stabilization and apoptosis resulting from ribosome biogenesis inhibition.<sup>20</sup> Importantly, all three components of the 5S RNP are dependent on each other to bind Hdm2 and as such, reduced uL18 or uL5 in several models fails to induce p53 stabilization to the same extent as the loss of other RPs.<sup>21-24</sup>

Symportin 1 (Syo1, HEATR3 in human) is a yeast protein that co-imports uL5 and uL18 into the nucleus.<sup>25,26</sup> Syo1 associates co-translationally with the N-terminus of uL18 and interacts with uL5, allowing for synchronized nuclear import of the newly synthesized RPs.<sup>25,26</sup> Once in the nucleus, a pre-5S RNP is formed by the incorporation of 5S rRNA with Syo1-uL18-uL5, which is then recruited onto the pre-60S large ribosomal subunit.<sup>27</sup> While co-immunoprecipitation experiments in human cells have recently shown that HEATR3 associates with both uL5 and uL18,<sup>28</sup> it remains unknown if the co-translational capture is conserved.

This study reports missense and splice site variants in *HEATR3* [MIM 614951] in multiple individuals presenting with DBA and additional clinical features. Functional studies reveal defective ribosome biogenesis, reduced nuclear import of uL18/RPL5, and suggest that the impaired erythroid proliferation is independent of p53.

## METHODS

**Affected individuals.** The exome sequencing results from Family A were brought to the attention of the European Diamond-Blackfan anemia (EuroDBA) consortium. This led to EuroDBA members querying their respective registries and the identification of the other families (see Supplementary Methods). Written informed consent was obtained from affected individuals and/or parents prior to inclusion in this study, which was performed in accordance with the ethical standards of the Declaration of Helsinki. All procedures in P3 were performed according to standards of institutional and national ethical boards (Hacettepe University: GO15/721, GO19/604). P4 and his family were registered in the French DBA registry (CNIL acceptance N°911387, CCTIRS-N°11.295, 12/05/2011).

**Cell culture.** Lymphoblastoid cell lines (LCLs) were derived from EBV-immortalization of peripheral mononuclear cells isolated from whole blood using Ficoll (GE Life Sciences) and grown in RPMI (Gibco) containing 10% or 15% fetal calf serum (FCS), 1% L-glutamine, and 1% penicillin/streptomycin. Fibroblasts were generated by a skin biopsy from the hip while the individual was anesthetized for a bone marrow biopsy and maintained in DMEM (Gibco) containing 10% fetal calf serum. HeLa cells were cultured in DMEM supplemented with 10% fetal bovine serum (Gibco).

**Erythroid cell culture assays.** Erythroid cell culture assays were performed as previously described.<sup>16,17,29</sup> Antibodies and stains for FACS analysis were PC7 or PE conjugated CD34 (Beckman Coulter), APC conjugated CD36 (BD Biosciences), APC or PE conjugated Band 3 (kindly provided by Mohandas Narla, NYBC or IBGRL, The international Blood group reference laboratory), PE/Cy7 conjugated IL-3R (Miltenyi Biotech), PE/Cy7 (PE)-coupled GPA (Life Technologies), and 7AAD (Miltenyi Biotech). FACS analysis was conducted on an Influx flow cytometer (BD Biosciences). Data were analyzed using Kaluza software (Beckman Coulter).

**Data Sharing Statement.** Disease-causing *HEATR3* variants have been submitted to ClinVar with accession numbers SCV002003962, c.1751G>A p.(Gly584Glu), homozygous P1 and P2 ; SCV001983775, c.1337G>A p.(Cys446Tyr), homozygous P3 ; SCV002059206, c.399+1G>T p.? and SCV002059215, c.719C>T p.(Pro240Leu), compound heterozygous P4; SCV001976527, c.400T>C p.(Cys134Arg), homozygous P5 and P6. Data supporting the findings of this study are available upon request.

## RESULTS

### Variants in *HEATR3* drive hematological phenotypes with additional clinical features

Two of three children from Family A, P1 and P2, presented with intellectual disability (ID), bone marrow failure with marked erythroid-lineage involvement, short stature as well as some minor facial and acromelic findings such as synophrys, pes planus, hallux valgus and brachydactyly (Table 1 and Figure 1A,B). The elder sister, P1, died of osteosarcoma at age 20. Initial whole exome sequencing (WES) of the parents and affected children pointed to five candidate genes with either homozygous or compound heterozygous variants (Table S1). *HEATR3* [MIM 614951] was the most likely candidate due to its potential role in ribosome biogenesis.<sup>25</sup> *HEATR3* (NM\_182922) variant c.1751G>A; p.(Gly584Glu) was heterozygous in both parents and homozygous in P1 and P2. Subsequent Sanger sequencing DNA from whole blood of the unaffected child revealed a heterozygous *HEATR3* variant. Based on the hematological phenotype found in P1 and P2, all five candidate genes including *HEATR3* were reported to the European Diamond-Blackfan Anemia consortium (EuroDBA).

Queries into the Turkey EuroDBA registry revealed a second consanguineous family with an affected child and three siblings, two of whom died in early childhood (Family B). The affected child, P3, had ID, pure erythroid hypoplasia, short stature and some minor dysmorphic findings overlapping with those of P1 and P2 (Table 1 and Figure 1A,B). A focus on the five candidate genes in WES (Table S1) revealed a homozygous c.1337G>A; p.(Cys446Tyr) variant in *HEATR3*, supporting the findings in Family A. A similar screening of the French DBA registry identified a compound heterozygous variant in *HEATR3* that coupled a canonical splice-site variant c.399+1G>T with a missense variant c.719C>T; p.(Pro240Leu), which segregate from either parent (Family C). In marked contrast to Families A and B, the affected individual in

Family C, P4, had no ID or dysmorphic findings, but had short stature, pure erythroid hypoplasia and interatrial septal defect (ostium secundum) (Table 1).

Finally, a fourth family of Dutch origin was identified with *HEATR3* variants. The eldest sister (P5) presented with a severe anemia, ID, operated preaxial polydactyly in the right hand and clinodactyly of the left thumb, mild facial dysmorphic features, and congenital hip dysplasia (Table 1 and Figure 1A,B). The brother (P6) had anemia and transient thrombocytopenia with mild dysmorphic facies and no ID (Figure 1A,B). WES in P5 identified the homozygous c.400T>C; p.(Cys134Arg) variant in *HEATR3*. Sanger sequencing revealed this homozygous *HEATR3* variant in P6, and a heterozygous variant was found in both parents. This variant is predicted to be “deleterious” according to SIFT and “disease-causing” by Mutation Taster, but not predicted to impact splicing according to HSF, MaxEntScan, and NNSPLICE.<sup>30–34</sup> None of these variants were found in the gnomAD, except for the c.400T>C; p.(Cys134Arg) variant in Family D which is very rare with an allele frequency of  $4.11 \times 10^{-6}$  and not present in homozygosity.<sup>35</sup>

At the amino acid level, all these human variants occur at positions which are highly conserved evolutionarily (Figure S1). Sanger sequencing performed on DNA extracted from lymphoblastoid cell lines (LCLs) (in case of P2 and P3), isolated lymphocytes (P4) and peripheral blood (P5 and P6) confirmed the expected *HEATR3* variants (Figure 1C). These variants are found dispersed across *HEATR3* with no apparent clustering except that they all affect residues in the ARM and HEAT repeat domains of the *HEATR3* protein (Figure 1D,E). In order to exclude other biallelic genomic variants, common long contiguous stretches of homozygosity (LCSH) >5Mbp were identified for individuals P1, P2, P3 and P5, which revealed a single common LCSH on chromosome 16 ([GRCh37] 25,263,278-53,191,470) where *HEATR3* lies (Figure S2).

### The HEATR3 p.Gly584 (yeast p.Gly522) residue is important for protein function

In budding yeast, Syo1 is important for 60S ribosomal subunit assembly.<sup>25</sup> Figure S1 illustrates the amino acids affected by the four human variants, highlighting that only p.Gly584 has a homologous residue in yeast Syo1, p.Gly522. In order to test the effects of the p.Gly584 HEATR3 mutation, we engineered suitable yeast strains. Yeast cells with deletions in *syo1* (*syo1Δ*) are viable but display a mild growth defect (Figure 2B, apparent at 10<sup>3</sup>x and higher dilutions in a plate assay), and a striking accumulation of 40S subunits (Figure 2A). The p.Gly584 HEATR3 residue was mutated in yeast Syo1 to yield p.(Gly522Ala) to probe function, or p.(Gly522Glu) to mimic the variant in P1 and P2. Expression of the mutated constructs did not restore growth (Figure 2B) or the ribosomal subunit imbalance (Figure 2A). By comparison, introduction of wild-type Syo1 complemented both growth and ribosomal subunit accumulation (Fig 2A,B). Western blot analysis revealed that neither variant had a noticeable impact on protein abundance (Figure 2C). Mapping the human p.Gly584 residue onto the *Chaetomium thermophilum* Syo1 3-D structure, established in complex with uL18 by X-ray crystallography,<sup>25</sup> reveals the presence of the equivalent p.Gly580 amino acid in an  $\alpha$ -helix at a distance from the contacts with the ribosomal protein. This suggests the pathogenicity of the HEATR3 p.(Gly584Glu) variant is linked to efficient 60S ribosomal subunit production.

To establish if the co-translational capture of uL18 by Syo1<sup>25,26</sup> is conserved in higher eukaryotes, we transiently expressed HA-tagged HEATR3 in HeLa cells, stalled ribosomes with cycloheximide, and performed an anti-HA affinity purification. The recovered material was tested for the presence of *RPL5* mRNAs (coding for uL18) by RTqPCR. Compared to an untagged HEATR3 control, *RPL5* mRNA was found significantly enriched in HA-HEATR3 pellets (Figure S3). No co-translational recruitment of *RPL5* mRNA was observed when the HA-HEATR3

p.(Cys446Tyr) variant was expressed (Figure S3). We also tested for the presence of *RPL10* mRNA coding for uL16, an RP that is not known to be chaperoned by Syo1.<sup>26</sup> Consistently, we detected no signal in the HA-HEATR3 or in the untagged control pellets for *RPL10* (Figure S3). We conclude that the co-translational capture mechanism used by yeast Syo1 to chaperone uL18 is conserved by HEATR3 in human cells, and disrupted by the HEATR3 p.(Cys446Tyr) variant.

### ***HEATR3* missense variants destabilize the HEATR3 protein and reduce nuclear uL18**

To assess the effects of patient mutations on HEATR3 metabolic stability, protein levels were established by western blotting using lysates from LCLs derived from P2 and P3. The HEATR3 protein was barely detectable in either of the affected samples compared to the healthy controls (Figure 3A). To determine if this effect was due to the variants driving constitutive ubiquitin-mediated degradation of HEATR3 (similar to the fate of p53 in LCL basal conditions<sup>24</sup>), cells were exposed to the proteasome inhibitor MG-132 and blotted again for HEATR3. No restoration of HEATR3 levels was observed upon MG-132 treatment, in contrast to the clear and expected increase of p53 protein (Figure 3A). This reduction of HEATR3 protein was not due to a loss of *HEATR3* transcription, as real-time qPCR analysis revealed equivalent levels of *HEATR3* mRNA in cells from healthy and affected individuals (Figure 3B). These results suggest that the *HEATR3* variants p.(Cys446Tyr) and p.(Gly584Glu) trigger the destabilization of the protein independently of the proteasome and without affecting *HEATR3* mRNA levels.

To test if the uL18-nuclear-import role of Syo1<sup>25</sup> is conserved in human cells, *HEATR3* expression was knocked down with siRNAs in HeLa cells (Figure 3C) and stained with antibodies recognizing uL18. Figure 3D shows that in control cells, uL18 accumulated in the cytoplasm and the nucleus with a particularly strong enrichment in the nucleolus (where

ribosome biogenesis initiates). Upon depletion of HEATR3, this enrichment of uL18 was lost in nearly all cells.

To confirm this finding in primary patient cells, dermal fibroblasts were obtained from P2. Figure 3E shows nuclear staining of uL18 in fibroblasts expressing the HEATR3 variant p.(Gly584Glu) is reduced compared to control cells (quantification, Figure 3F). Staining the depleted HeLa cells (data not shown) or fibroblasts (Figures 3E,F) with antibodies recognizing uL5 (RPL11) did not reveal any appreciable differences. We thus conclude that HEATR3 is important for nuclear import of uL18 and that uL5 appears to be imported through additional mechanisms.

### **Cells carrying *HEATR3* variants reveal strong pre-rRNA processing defects**

Northern blot analysis of total RNA extracts compared pre-rRNA processing in LCLs generated from three affected individuals and three healthy controls. A striking common feature of the profiles of affected individuals was the accumulation of 32S pre-rRNAs, and to a lesser extent of the 12S pre-rRNA (Figure 4A, 4C, ITS2 probe). Quantitative analyses of precursor to product ratios for the affected individuals relative to controls (RAMP<sup>36</sup>) showed a strong increase of 32S/41S ratios and a decrease of 12S/32S ratios (Figure 4B). This suggests a delayed endonucleolytic cleavage at site 4 in the internal transcribed spacer 2 (ITS2), which separates the 5.8S and the 28S rRNAs on the primary transcript. These results are reminiscent of similar accumulations of 32S pre-rRNA in LCLs from *RPL5*<sup>+/*mut*</sup> and *RPL11*<sup>+/*mut*</sup> individuals presenting with DBA.<sup>37</sup>

To prove these processing defects are truly due to loss of *HEATR3*, we conducted complementation assays in LCLs cells. Expression of wild-type *HEATR3* cDNA in patient LCLs (P3) by lentiviral infection was sufficient to restore normal pre-rRNA processing (Figure 4C,D). In

line with these results, acute depletion of HEATR3 in U2OS and HCT116 cells displayed similar changes in the pre-rRNA processing pattern (notably 32S accumulation, Figure S4).

### **The levels of 60S ribosomal subunits are reduced in cells with *HEATR3* variants**

The impact of these pre-rRNA processing impairments on 60S ribosomal subunit formation was measured by subjecting the same LCLs to polysomal profiling. As in yeast, we found that LCLs carrying *HEATR3* variants revealed a substantial loss of free 60S ribosomal subunits (Figure 5A,B). Also evident was a loss of 80S monosomes, which would be expected upon a 60S subunit shortage. These profiles are reminiscent of LCLs from individuals with DBA who carry variants in *RPL* genes.<sup>38–40</sup> Expressing wild-type *HEATR3* cDNA in patient LCLs (P3) with lentiviruses was sufficient to restore normal levels of 60S subunits (Figure 5B). Taken altogether, the results demonstrate that variants in *HEATR3* have a major impact on the biogenesis of 60S ribosomal subunits.

### **Variants or reductions in *HEATR3* affect erythropoiesis**

As part of a more complete hematological evaluation, bone marrow smears of P2 and P5 were examined. The results revealed erythroblastopenia that was associated with hypolobulated megakaryocytes that retained a normal size, excluding dysmegakaryopoiesis (Figure 6A and Table 2). The erythroid cell cultures of CD34<sup>+</sup> cells purified from bone marrow of P2 revealed severe defects in erythroid cell proliferation compared to a healthy control (Figure 6B). Comparing differentiation markers of P2 and healthy control cells in this assay by flow cytometry suggests that there were no detectable differences in erythroid precursor mortality (7AAD labelling) or in IL3R<sup>neg</sup>, CD34<sup>neg</sup>/CD36<sup>+</sup> expression levels at day 7 (Figure S5A). However, we observed a higher proportion of basophilic (both early and late) and orthophilic cells relative to proerythroblasts at day 10 and 12 in P2 cells, suggesting an acceleration of the terminal

differentiation program (Figure 6C,D). This may be correlated to the increased Band 3 expression at day 10 in P2 compared to the healthy control (Figure S5B,C). A similar assay was performed with CD34<sup>+</sup> cells purified from peripheral blood of P4, both parents of P4, and a healthy control. As with P2, a strong defect in erythroid cell proliferation was observed in the cells derived from P4 (Figure S5E).

To confirm the findings in Figure 6, erythroid cell culture assays were performed with CD34<sup>+</sup> cells purified from cord blood and transduced with lentiviruses expressing shRNAs targeting *HEATR3* that reduced transcript levels (Figure 6E). CD34<sup>+</sup> cells infected with these shRNAs revealed a dramatic decrease in erythroid proliferation compared to cells transduced with a scrambled control shRNA (Figure 6F). While *HEATR3* knockdown led to similar proportions of CD34<sup>+</sup>/CD36<sup>neg</sup> (BFU-E) cells, the increased proportion of CD34<sup>neg</sup>/CD36<sup>+</sup> (CFU-E) at day 7 and day 10 compared to control (Figure S6) also suggests an acceleration of erythroid maturation. No apoptosis was observed, levels of the p53 target p21 and procaspase 3 proteins were unchanged (Figure 6G). No significant differences in expression of ILR3<sup>neg</sup> were detected (data not shown), and levels of eS19 (RPS19), HSP70 and GATA1 were similarly equivalent in control and *HEATR3* shRNA-expressing cells (Figure 6G). Some caution may be warranted in interpreting the western blot results given the different phases of maturation that the control vs. *HEATR3* knockdown cells reveal on the days collected for analysis.

### ***HEATR3* variants do not alter levels of p53, uL5, or uL18 in LCLs**

To confirm that p53 is not stabilized in cells with *HEATR3* loss, western blot analysis was performed with lysates from patient LCLs. Blotting for p53 reveals that *HEATR3* variants do not drive p53 stabilization (Figures 7A,B). Similarly, depletion of *HEATR3* in U2OS or HCT116 cells also does not lead to p53 stabilization (Figure S4A). The p53 response to a DNA damaging agent (camptothecin) or a proteasomal inhibitor (MG-132) was normal in patient LCLs (Figure

7A,B). No difference was detected in the total levels of uL5 or uL18 in LCLs carrying *HEATR3* variants, suggesting that the nuclear reductions of uL18 observed in Figure 3 are not due to uL18 loss.

## DISCUSSION

We have identified *HEATR3* as a novel causative gene of DBA in four distinct families with members carrying biallelic variants. While DBA has been associated to date with at least 23 of the total 80 human RP genes,<sup>41</sup> the number of non-RP genes driving this disorder remain far lower.<sup>1-4</sup> We demonstrate that these *HEATR3* variants drive classical DBA through a distinctive effect on ribosome biogenesis, whereupon reduced nuclear import of uL18 impairs production of 60S ribosomal subunits.

From a clinical perspective, the syndrome linked to *HEATR3* mutations manifests as a variant form of DBA with additional features. Hematologically, the patients were all normocytic at diagnosis. Two patients were found to have thrombocytopenia at some stage, but it was transient in one patient (P6) and related to chemotherapy for osteosarcoma treatment in another (P1). Three out of six patients are transfusion dependent, two need no treatment at all, and one patient is treated with corticosteroids, suggesting that, in agreement with our general knowledge of DBA, the hematological phenotype is heterogeneous and patients may become treatment independent.<sup>43</sup> ID is rarely reported in classical DBA, and the few described cases are mostly linked to microdeletions that are considered to be driving a contiguous gene syndrome (unlike the individuals here).<sup>41</sup> In contrast, other associated clinical features such as growth retardation (four of six individuals) and acromelic dysmorphic features (five of six individuals) are commonly reported in DBA.<sup>44</sup> We observed a higher frequency of skeletal abnormalities (in 5/6, 83%) and

facial dysmorphism (in 5/6, 83%), compared to congenital malformations in ~ 50% of all DBA patients<sup>44</sup>. Interestingly, the abnormal thumb defect that is often reported in DBA patients with *RPL5* variants<sup>37</sup> is also observed in a majority of the patients with *HEATR3* variants. In addition, 4/6 (60%) were diagnosed with (truncal) obesity, which was not treatment-related in three patients. Of note, P4 suffered from unexplained severe diarrhea and colitis mimicking Crohn's disease (Table 1). Interestingly, the *HEATR3* allelic variation leading to the amino acid change p.(Arg642Ser) has been reported associated with Crohn's disease in the Ashkenazi Jewish population.<sup>45</sup>

All reported pathogenic ribosome-related gene variants in DBA are inherited dominantly.<sup>42,44</sup> The only exception to this is the X-linked recessive hypomorphic variant in *TSR2*, a gene that codes for a pre-rRNA processing protein that contributes to ribosome biogenesis by promoting the assembly of RPS26/eS26.<sup>3</sup> *HEATR3* is the second gene after *TSR2* coding for a ribosome biogenesis factor linked to DBA and interestingly, the *HEATR3* variants are also inherited in a recessive manner. Ribosome biogenesis factors are not integral components of the ribosomes, they interact transiently with maturing precursor subunits to promote numerous assembly reactions. Most of these *trans*-acting factors are essential, and some are thought to recycle upon function completion.<sup>46</sup> Thus, ribosome biogenesis factors could be high-priority candidate genes for screening DBA families with recessive inheritance patterns.

The pathophysiology experiments reported here suggest that the variants p.(Cys446Tyr) and p.(Gly584Glu) impair the metabolic stability of the *HEATR3* protein (Figure 3). This loss of protein very likely underlies the reduction of nuclear uL18 observed in cells with the p.(Gly584Glu) variant (Figure 3F) and in HeLa cells with knocked down *HEATR3* (Figure 3C,E). This loss of uL18 accumulation in the nucleus is likely driving the impaired ribosome biogenesis observed in Figures 4 and 5. Despite this evident pre-rRNA processing defect, the ratio of

mature 28S/18S rRNAs was only slightly impacted in patient cells, in line with what was previously observed with DBA-linked RP gene variants<sup>38-39</sup>. But unlike knockdown of DBA-linked ribosomal proteins, the mature rRNA ratio was also not severely affected upon severe depletion of *HEATR3* in cell lines (Figure S4), indicating that *HEATR3* is a facilitator of ribosome biogenesis but it is not essential for the process. Similarly, *Syo1* in yeast is dispensable for cell viability and its deletion only marginally affects cell growth (Figure 2B). The perturbation resulting from *HEATR3* loss in patient cells is nonetheless sufficient to cause a significant deficit of 60S subunits (Figure 5), which may alter the dynamics of translation and affect synthesis of proteins essential to erythroid differentiation.

Along the same line, an important finding of this work is that knocking down *HEATR3* in CD34<sup>+</sup> cells, or other cell lines, does not trigger p53 stabilization or upregulation of its target p21 (Figures 6G and S4A). Accordingly, patient LCLs with *HEATR3* variants showed no increase of basal p53 levels (Figure 7A,B), unlike what is observed in most LCLs derived from patients carrying RP gene variants.<sup>47</sup> Indeed, nucleolar surveillance leading to p53 stabilization requires the nuclear accumulation of uL18,<sup>20</sup> the precise step impaired by *HEATR3* loss. Similar to our observations with *HEATR3*, *RPL5* knockdown in cell lines does not stabilize p53 and LCLs from DBA patients carrying *RPL5* variants do not reveal increased levels of p53.<sup>20,47</sup> This suggests a shared pathophysiological pathway between *HEATR3* variants and one of the most commonly mutated *RPL* genes in DBA (*RPL5*). These in vitro data do not exclude a role for p53 in vivo and future work is still required for a full understanding of how *HEATR3* deficiency leads to DBA.

One individual of this study (P1) died of osteosarcoma at age 20, suggesting that *HEATR3* may be a tumor suppressor gene. This would agree with previous studies pointing to a tumor suppressor role for *RPL5*.<sup>48</sup> Moreover, it has been reported that variants at the chromosomal locus 16q12.1 where *HEATR3* resides have significant risk associations with several cancers

including glioblastoma (rs10852606, the risk allele “C” is associated with reduced *HEATR3* expression), testicular (rs8046148 and rs10852606), and esophageal cancers (rs4785204 and rs4785204).<sup>49-51</sup> Further investigation is warranted, given the low number of individuals in this study.

We conclude that recessive loss-of-function variants in *HEATR3* drive a pathogenic phenotype in humans that includes classical DBA with dysmorphic features and ID. This study shows that *HEATR3* variants impair pre-rRNA processing and ribosome biogenesis by abrogating the co-translational capture and nuclear import of uL18, an ancient and conserved function of the yeast ortholog Syo1. The hematological defects linked to these variants appear to be caused by an abnormal acceleration of erythrocyte maturation coupled to a loss of proliferation capacity, and not by the stabilization of p53 or other known mechanisms driving DBA. This study adds a new disorder to the growing catalog of human ribosomopathies that drive blood disease.

## ACKNOWLEDGEMENTS

Our most special thanks go to the affected individuals, their families, and to the DBA patient associations. We would like to thank all the people involved in the mutational screening analysis in France (Christine Bole and the Team from the Genomics Core Facility, Institut Imagine-Structure Fédérative de Recherche Necker and technicians from the Hematology lab in R. Debré hospital, Paris), in Turkey (Z. Ekim Taskiran for facilitating WES studies in Hacettepe University Exome Facility and Can Kosukcu for obtaining WES data), and to the registry data manager Isabelle Marie in France. We would also like to thank Dr. Dirk Lebrecht and Marco Teller at the University Medical Center Freiburg for the generation of the LCLs, also Patricia Veltman and Petra Mooyer at the Laboratory of Genetic Metabolic Disease at the Amsterdam University Medical Center for the generation of the fibroblasts. We are grateful for the expert

assistance of Alexia Zakaroff and Elodie Riant (Genotoul-TRI, I2MC, Toulouse) to perform cell sorting, and Frédéric Martins and Emeline Lhuillier (Genotoul-GET Santé, I2MC, Toulouse) for ddPCR. Specific E-Rare grants funding EuroDBA researchers are as follows: ZonMW #40-44000-98-1008 in the Netherlands (AWM); TUBITAK 315S192 in Turkey (SU); #ANR-15-RAR3-0007-04 (PEG and MOD) and #ANR EJPRD/ANR-19-RAR4-0016 (LDC) in France. In addition, this project has received funding from the European Union's Horizon 2020 research and innovation programme under the EJP RD COFUND-EJP N° 825575. Specific grants under the frame of EJP RD programme JTC 2019 RiboEurope project are as follows: TUBITAK 319S062 in Turkey (AC); (EJP RD/JTC2019/PINT-MULTI) grant n°R.8015.19 and PDR grant n°T.0144.20] in Belgium. PEG, MFOD, and LDC are also funded by ANR-2015-AAP générique-CE12 (DBA-Multigenes). LDC is additionally supported by the Laboratory of Excellence for Red Cells [(LABEX GR-Ex)-ANR Avenir-11-LABX-0005-02], and The French National PHRC OFABD (DBA registry). DLJL is supported by the Belgian Fonds de la Recherche Scientifique (F.R.S./FNRS), the Université Libre de Bruxelles (ULB), the Région Wallonne (SPW EER) ["RIBO*cancer*" FSO grant n°1810070; POC grant n°1880014], the Fonds Jean Brachet, the Internationale Brachet Stiftung, and the Epitrans COST action (CA16120). KDK is supported by funding from the Foundation against Cancer (P2016-081 and 2016-112) and SV is a PhD fellow at FWO (1S49817N).

## **AUTHORSHIP CONTRIBUTIONS**

Involved in the clinical care and molecular diagnosis of the individuals in the study: S.U., P.O.S.K, N.Y, A.C, N.A.A., L.D.C., M.B., E.B., K.V.G., M.S.V., K.D.K., S.V., V.L., T.L.

Designed the study: A.M.W., M.O.D., L.D.C., M.B., P.E.G., D.L.J.L.

Designed and performed experiments: M.O.D., M.L., C.J., M.S., S.L., L.W., N.L., E.L., N.M.L., J.P.

Analyzed and interpreted data: A.M.W., M.O.D., L.D.C., M.L., C.J., R.H.H., P.E.G., D.L.J.L.

Contributed to the preparation and critical reviewing of manuscript: S.U., A.C., N.A.A., M.O.D., L.D.C., M.B., K.D.K., V.L., P.E.G., D.L.J.L.

Drafted the manuscript: A.M.W.

Revised the manuscript: A.M.W., P.E.G., D.L.J.L.

All authors approved the final version of the manuscript.

## **CONFLICT OF INTEREST DISCLOSURE**

None.

## **REFERENCES**

1. Sankaran, V. G. et al. Exome sequencing identifies GATA1 mutations resulting in Diamond-Blackfan anemia. *J. Clin. Invest.* 122, 2439–2443 (2012).
2. Kim, A. R. et al. Functional Selectivity in Cytokine Signaling Revealed Through a Pathogenic EPO Mutation. *Cell* 168, 1053-1064.e15 (2017).
3. Gripp, K. W. et al. Diamond-Blackfan anemia with mandibulofacial dystostosis is heterogeneous, including the novel DBA genes TSR2 and RPS28. *Am. J. Med. Genet. A* 164A, 2240–2249 (2014).
4. Lee, P. Y. Vasculopathy, immunodeficiency, and bone marrow failure: the intriguing syndrome caused by deficiency of adenosine deaminase 2. *Front. Pediatr.* 6, 282 (2018).

5. Lipton, J. M. & Ellis, S. R. Diamond-Blackfan Anemia: Diagnosis, Treatment, and Molecular Pathogenesis. *Hematol Oncol Clin North Am.* 23, 261–282 (2009).
6. Vlachos, A., Rosenberg, P. S., Atsidaftos, E., Alter, B. P. & Lipton, J. M. Incidence of neoplasia in Diamond Blackfan anemia: A report from the Diamond Blackfan anemia registry. *Blood* 119, 3815–3819 (2012).
7. Bolze, A. et al. Ribosomal protein SA haploinsufficiency in humans with isolated congenital asplenia. *Science* 340, 976–978 (2013).
8. Paolini, N. A. et al. A Ribosomopathy Reveals Decoding Defective Ribosomes Driving Human Dysmorphism. *Am. J. Hum. Genet.* 100, 506–522 (2017).
9. Gong, X. et al. An investigation of ribosomal protein L10 gene in autism spectrum disorders. *BMC Med. Genet.* 10, 7 (2009).
10. Brooks, S. S. et al. A novel ribosomopathy caused by dysfunction of RPL10 disrupts neurodevelopment and causes X-linked microcephaly in humans. *Genetics* 198, 723–733 (2014).
11. Thevenon, J. et al. RPL10 mutation segregating in a family with X-linked syndromic Intellectual Disability. *Am. J. Med. Genet. Part A* 167, 1908–1912 (2015).
12. Dutt, S. et al. Haploinsufficiency for ribosomal protein genes causes selective activation of p53 in human erythroid progenitor cells. *Blood* 117, 2567–2576 (2011).
13. Ellis, S. R. Nucleolar stress in Diamond Blackfan anemia pathophysiology. *Biochim. Biophys. Acta* 1842, 765–768 (2014).
14. Horos, R. et al. Ribosomal deficiencies in Diamond-Blackfan anemia impair translation of transcripts essential for differentiation of murine and human erythroblasts. *Blood* 119, 262–272 (2012).
15. Cheng, Z. et al. Small and Large Ribosomal Subunit Deficiencies Lead to Distinct Gene Expression Signatures that Reflect Cellular Growth Rate. *Mol. Cell* 73, 36–47.e10 (2019).

16. Rio, S. et al. Regulation of globin-heme balance in Diamond-Blackfan anemia by HSP70/GATA1. *Blood* 133, 1358–1370 (2019).
17. Gastou, M. et al. The severe phenotype of Diamond-Blackfan anemia is modulated by heat shock protein 70. *Blood Adv.* 1, 1959–1976 (2017).
18. Ciganda, M. & Williams, N. Eukaryotic 5S rRNA biogenesis. *Wiley Interdiscip Rev RNA* 2 523–533 (2011).
19. Donati, G., Peddigari, S., Mercer, C. A. & Thomas, G. 5S Ribosomal RNA Is an Essential Component of a Nascent Ribosomal Precursor Complex that Regulates the Hdm2-p53 Checkpoint. *Cell Rep.* 4, 87–98 (2013).
20. Nicolas, E. et al. Involvement of human ribosomal proteins in nucleolar structure and p53-dependent nucleolar stress. *Nat. Commun.* 7, 11390 (2016).
21. Nieto Bernáldez, B. et al. Efficient fractionation and analysis of ribosome assembly intermediates in human cells. *RNA Biol.* 18(sup1), 182-197 (2021).
22. Fumagalli, S., Ivanenkov, V., Teng, T. & Thomas, G. Suprainduction of p53 by disruption of 40S and 60S ribosome biogenesis leads to the activation of a novel G2/M checkpoint. *Genes Dev.* 26, 1028–1040 (2012).
23. Teng, T., Mercer, C. A., Hexley, P., Thomas, G. & Fumagalli, S. Loss of tumor suppressor RPL5/RPL11 does not induce cell cycle arrest but impedes proliferation due to reduced ribosome content and translation capacity. *Mol. Cell. Biol.* 33, 4660–4671 (2013).
24. Pereboom, T. C. et al. Translation of branched-chain aminotransferase-1 transcripts is impaired in cells haploinsufficient for ribosomal protein genes. *Exp. Hematol.* 42, 394-403.e4 (2014).
25. Kressler, D. et al. Synchronizing nuclear import of ribosomal proteins with ribosome assembly. *Science* 338, 666–671 (2012).

26. Pausch, P. et al. Co-translational capturing of nascent ribosomal proteins by their dedicated chaperones. *Nat. Commun.* 6, 7494 (2015).
27. Calviño, F. R. et al. Symportin 1 chaperones 5S RNP assembly during ribosome biogenesis by occupying an essential rRNA-binding site. *Nat. Commun.* 6, 6510 (2015).
28. Hannan, K. M., Soo, P., Wong, M. S., Lee, J. K. & Hein, N. Nuclear stabilisation of p53 requires a functional nucleolar surveillance pathway. *bioRxiv* 2021.01.21.427535 (2021).
29. Hu, J. et al. Isolation and functional characterization of human erythroblasts at distinct stages: implications for understanding of normal and disordered erythropoiesis in vivo. *Blood* 121, 3246–3253 (2013).
30. Reese, M. G. Improved splice site detection in Genie. in *Journal of Computational Biology* 4, 311–323 (1997).
31. Yeo, G. & Burge, C. B. Maximum entropy modeling of short sequence motifs with applications to RNA splicing signals. *J. Comput. Biology* 11, 377–394 (2004).
32. Desmet, F. O. et al. Human Splicing Finder: An online bioinformatics tool to predict splicing signals. *Nucleic Acids Res.* 37, e67 (2009).
33. Schwarz, J. M., Cooper, D. N., Schuelke, M. & Seelow, D. Mutationtaster2: Mutation prediction for the deep-sequencing age. *Nat. Methods* 11, 361–362 (2014).
34. Sim, N. L. et al. SIFT web server: Predicting effects of amino acid substitutions on proteins. *Nucleic Acids Res.* 40, W452-457 (2012).
35. Karczewski, K. J. et al. The mutational constraint spectrum quantified from variation in 141,456 humans. *Nature* 581, 434–443 (2020).
36. Wang, M., Anikin, L. & Pestov, D. G. Two orthogonal cleavages separate subunit RNAs in mouse ribosome biogenesis. *Nucleic Acids Res.* 42, 11180–11191 (2014).
37. Gazda, H. T. et al. Ribosomal Protein L5 and L11 Mutations Are Associated with Cleft Palate and Abnormal Thumbs in Diamond-Blackfan Anemia Patients. *Am. J. Hum. Genet.* 83, 769–780 (2008).

38. Wlodarski, M. W. et al. Recurring mutations in RPL15 are linked to hydrops fetalis and treatment independence in diamond-blackfan anemia. *Haematologica* 103, 949–958 (2018).
39. Lezzerini, M. et al. Ribosomal protein gene RPL9 variants can differentially impair ribosome function and cellular metabolism. *Nucleic Acids Res.* 48, 770–787 (2020).
40. Ludlow, A. et al. The Use of B-Cell Polysome Profiling to Validate Novel RPL5 (uL18) and RPL26 (uL24) Variants in Diamond-Blackfan Anemia. *J. Pediatr. Hematol. Oncol.* 43, e336-e340 (2020)
41. Da Costa, L. et al. Molecular approaches to diagnose Diamond-Blackfan anemia: The EuroDBA experience. *Eur. J. Med. Genet.* 61, 664–673 (2018).
42. Costa, L. Da, Leblanc, T. & Mohandas, N. Diamond-Blackfan anemia. *Blood* 136, 1262–1273 (2020).
43. Vlachos, A. & Muir, E. How I treat Diamond-Blackfan anemia. *Blood* 116, 3715–3723 (2010).
44. Ulirsch, J. C. et al. The Genetic Landscape of Diamond-Blackfan Anemia. *Am. J. Hum. Genet.* 103, 930–947 (2018).
45. Zhang, W. et al. Extended haplotype association study in Crohn's disease identifies a novel, Ashkenazi Jewish-specific missense mutation in the NF- $\kappa$ B pathway gene, HEATR3. *Genes Immun.* 14, 310–316 (2013).
46. Peña, C., Hurt, E. & Panse, V. G. Eukaryotic ribosome assembly, transport and quality control. *Nat. Struct. Mol. Biol.* 24, 689–699 (2017).
47. Aspesi, A. et al. Lymphoblastoid cell lines from Diamond Blackfan anaemia patients exhibit a full ribosomal stress phenotype that is rescued by gene therapy. *Sci. Rep.* 7, 12010 (2017).

48. Fancello, L., Kampen, K. R., Hofman, I. J. F., Verbeeck, J. & De Keersmaecker, K. The ribosomal protein gene RPL5 is a haploinsufficient tumor suppressor in multiple cancer types. *Oncotarget* 8, 14462–14478 (2017).
49. Ruark, E. et al. Identification of nine new susceptibility loci for testicular cancer, including variants near DAZL and PRDM14. *Nat. Genet.* 45, 686–689 (2013).
50. Melin, B. S. et al. Genome-wide association study of glioma subtypes identifies specific differences in genetic susceptibility to glioblastoma and non-glioblastoma tumors. *Nat. Genet.* 49, 789–794 (2017).
51. Wu, C. et al. Genome-wide association analyses of esophageal squamous cell carcinoma in Chinese identify multiple susceptibility loci and gene-environment interactions. *Nat. Genet.* 44, 1090–1097 (2012).

Clinical Findings	P1	P2	P3	P4	P5	P6
Age at last visit	died at age 20y	10y	17y	11y	9y	5y
Sex	Female	Male	Male	Male	Female	Male
Ethnicity	Turkish	Turkish	Turkish	French	Dutch	Dutch
Country	Netherlands	Netherlands	Turkey	France	Netherlands	Netherlands
Family	A	A	B	C	D	D
Variant in <i>HEATR3</i> (ENST00000299192)	c.1751G>A p.(Gly584Glu) homozygous	c.1751G>A p.(Gly584Glu) homozygous	c.1337G>A p.(Cys446Tyr) homozygous	c.399+1G>T p.? heterozygous and c.719C>T p.(Pro240Leu) heterozygous	c.400T>C p.(Cys134Arg) homozygous	c.400T>C p.(Cys134Arg) homozygous
<b>Systemic Findings</b>						
Hematological findings at presentation	Anemia	Anemia	Anemia	Anemia	Anemia	Anemia and thrombocytopenia
Body mass index (normal 18.5-24.9)	29	23.7	28.1	18.7	22.8	16.3
Height	< -3 SD	< -1 SD	< -4 SD	< -1 SD (growth hormone therapy at 4y, < -3 SD at 2 mo)	< -1 SD	0 SD
Head Circumference	NA	Normal (0 SD)	< -3 SD	NA	> +1 SD	> +1 SD
Skeletal Findings	Brachydactyly of hands, Distal tapering of fingers, Pes planus, Hallux valgus	Pes planus, Hallux valgus of the left foot, Bilateral Hypoplasia of the 4th and 5th toes	Severe genu valgum (operated), Pes planus, Brachydactyly of hands, Hypoplasia of toes, Sandal gap, Cubitus valgus	None	Congenital hip dysplasia, Preaxial polydactyly of right hand (operated), Clinodactyly of left thumb, Brachydactyly of 1st metacarpals, Distal tapering of fingers	Brachydactyly of hands
Intellectual Disability/ Developmental Delay	Mild	Mild	Mild	None	Mild	None
Facial Dysmorphism	Synophrys, Hypertelorism, Low set ears	Coarse hair, Straight eyebrows, Synophrys, Protruding ears, Full cheeks, Narrow mouth	Down-slanted palpebral fissures, Mild ptosis of left eye, Widow's peak, Micrognathia, Protruding ears	None	Straight eyebrows	Down-slanted palpebral fissures, Low set ears
Skin Findings	None	Cutis marmorata	Multiple nevi, Facial freckling	Multiple nevi	None	None
Echocardiogram	NA	NA	Aortic regurgitation, dysplastic aortic valves	Interatrial septal defect (ostium secundum)	Normal	NA
Gastrointestinal Findings	None	None	None	Persistent diarrhea, Colitis	None	None
Other Findings	Obesity, PCOS, hypotonia	Truncal obesity, ENT problems	Truncal Obesity	None	Obesity	None
History of RBC Transfusion	Yes	No	Yes	Yes	Yes	Transient
Response to Corticosteroid	No	NA	Yes	No	NA	NA
Current Treatment	-	None	Corticosteroid	Transfusion and iron chelation	Transfusion and iron chelation	None
Clinical Course	Died of osteosarcoma at 20y	Currently in good clinical condition	Currently in good clinical condition	Currently in good clinical condition	Currently in good clinical condition	Currently in good clinical condition
<b>Family History</b>						
Consanguinity	First degree cousins	First degree cousins	First degree cousins	No	Likely	Likely
Family History	Yes, sibling (P1)	Yes, sibling (P2)	Yes, sibling	None	Yes, sibling (P6)	Yes, sibling (P5)

**Table 1. The clinical features of the individuals in this study.** SD: standard deviation. PCOS: polycystic ovarian syndrome. ENT: ears, nose, throat. NA: not available

Hematological findings		P1	P2	P3	P4	P5	P6						
<b>Blood Parameters</b>													
	Reference values	first available	most recent*	first available	most recent	first available	most recent	first available	most recent	first available	most recent	first available	most recent
Hemoglobin	age-dependent (g/dL)	6.8	7.2	10.5	10.3	7.4	10.1	3	8.1	4.5	7.1	5.6	9.4
Reticulocytes	25-120 (x 10 <sup>9</sup> /L)	108	NA	87.5	32.1	NA	96.9	decreased	7.2	NA	14	127	38
MCV	80-97 fL	84	86	81	78	88	94.8	NA	NA	NA	86.1	NA	80.4
Leukocytes	4.5-13 (x 10 <sup>9</sup> /L)	13.6	4.9	7.1	4.5	6.3	7.2	normal	7.2	10.9	5.5	5.3	8.1
Platelets	150-450 (x 10 <sup>9</sup> /L)	373	76	239	213	235	248	normal	220	269	288	< 10	193
HbF	<1% (after 1-2 year of age)	NA	NA	NA	3.3	NA	NA	NA	NA	NA	1.0	NA	1.4
eADA	<1.4 (U/g Hb)	NA	NA	8.3	NA	NA	12.8	NA	NA	NA	NA	NA	4.02
<b>Bone Marrow Findings</b>													
Erythroid lineage		Decreased		Decreased		Decreased		Decreased		Decreased		Decreased	
Dyserythropoiesis		No		No		No		No		No		No	
Megakaryocytic lineage		Normal		Normal		Normal		Normal		Normal		Normal	
Remarks				Some monolobulated megakaryocytes, normal size						Some monolobulated megakaryocytes, normal size			

\* during last phase treatment for osteosarcoma

**Table 2. Hematological features of the individuals in this study. NA: not available.**

## FIGURE LEGENDS

### Figure 1. Clinical presentation and *HEATR3* variants that drive DBA

**A)** Photographs of the face and hands of the affected individuals P1, P2, P3, P5 and P6 (photos from Family C not available). No common facial finding was present in affected individuals, but straight eyebrows, down-slanting palpebral fissures and synophrys are apparent in some. Note that fingers appear disproportionately short compared to hand in P1, P3 and P6. Also, note the presence of thumb anomaly in P5.

**B)** The pedigrees of Families A-D with genotypes for specified *HEATR3* variants are indicated below each available individual. The pathogenic variants are indicated in red.

**C)** *HEATR3* variants co-segregating with DBA in one affected individual from each family arranged according to position of coding sequence in ascending order. The missense variants c.400T>C (p.Cys134Arg) in P5; c.1337G>A (p.Cys446Tyr) in P3; c.1751G>A (p.Gly584Glu) in P1 and P2 are homozygous; while the splice donor site variant c.399+1G>T (p.?) and the missense variant c.719C>T (p.Pro240Leu) are compound heterozygous in P4.

**D)** Schematic representation of *HEATR3* with fifteen exons.

**E)** *HEATR3* protein with four ARM (Armadillo) and six HEAT (Huntingtin, Elongation factor 3, protein phosphatase 2A, and Target of rapamycin 1) repeat domains, indicating the position of associated variants. The protein domains were previously described.<sup>27,28</sup>

### Figure 2. The *HEATR3* Gly584 (yeast Gly522) residue is important for protein function

**A)** Polysome profiles of wild-type and *syo1Δ* yeast cells expressing empty vector controls or HA-tagged Syo1-Gly522 mutations display an altered 60S/40S subunits ratio. Representative examples of a duplicate are shown.

**B)** Mutations at position Gly522 do not complement yeast growth. The mild growth impairment observed in *syo1Δ* cells is complemented by a wild-type construct (HA-SYO) but not by

constructs harboring a mutation at position Gly522. The indicated strains were grown at 16°C on synthetic medium lacking leucine for 6 days.

**C)** The Gly522 mutants are stably expressed in yeast. HA-Syo1 constructs were detected by western blotting with an anti-HA antibody. As loading control, a GAPDH probing was performed.

**D)** Position of yeast mutation Gly522 on the 3-D structure of *Chaetomium thermophilum* Syo1 in complex with L5-N (based on PDB 4GMN<sup>25</sup>). Yeast Gly522 corresponds to Gly584 in the C-terminal (see Figure S1). Two views are shown.

### **Figure 3. HEATR3 variants affect protein levels and uL18 nuclear localization**

**A)** Representative western blot of lysates from LCLs derived from individuals P2 and P3 that were either untreated or exposed to the proteasome inhibitor MG-132. Specific antibodies are used to detect the relative amounts of HEATR3. Protein p53 provides a positive control showing proteasome inhibition by MG-132. Actin detection was used as loading control.

**B)** Real-time PCR analysis of cDNAs generated from LCLs derived from a healthy control or from patients P2 and P3 using primers to measure *HEATR3* mRNA levels. The mRNAs of genes *36B4*, *ACTB*, and *GAPDH* were used as references. Data shown are the results of six biological replicate experiments.

**C)** Western blot of lysates from HeLa cells transfected with two different siRNAs targeting *HEATR3* (#1 and #2) or a control scrambled siRNA (SCR) probed with antibodies against HEATR3. GAPDH detection was used as loading control.

**D)** Wide-field fluorescence microscopy of HeLa cells transfected with SCR or *HEATR3* siRNAs and stained with DAPI (to label the nucleus) and antibodies against uL18, shown at 20x magnification. The insets show enlarged pictures of the areas framed by dotted lines. The arrowheads point to stained nucleoli, which are observed in control cells but not after *HEATR3* knockdown.

**E)** Fibroblasts derived from a healthy control or the individual P2 stained with DAPI and antibodies against uL18 or uL5. Scale bar, 10  $\mu$ m.

**F)** Quantification of the number of fibroblasts revealing nuclear staining of uL18.

#### **Figure 4. Variants in *HEATR3* affect pre-rRNA processing**

**A)** Northern blot analysis of LCLs derived from control or affected individuals carrying *HEATR3* variants. Radiolabeled probes targeting the 5' extremity of ITS1 (5'ITS1), the ITS1/5.8S junction (ITS1-5.8S probe) or ITS2 were used to detect pre-rRNA precursors. Each lane was loaded with 3  $\mu$ g total RNA.

**B)** Quantification of pre-rRNAs in LCLs derived from individuals carrying *HEATR3* variants was performed by Ratio Analysis of Multiple Precursors (RAMP): product to precursor ratios at various processing steps are expressed as variations relative to LCLs from healthy controls. Mean values  $\pm$  s.e.m. from three independent experiments, aside from sample P4 for which n=2.

**C)** Restoration of *HEATR3* expression in LCLs from patient P3. LCLs from patient P3 and from a control individual were transduced with lentiviruses expressing either GFP (LV-GFP) or *HEATR3* (LV-*HEATR3*). Western-blot analysis confirmed expression of *HEATR3* in P3 LCLs transduced with LV-*HEATR3* (upper panel). Northern-blot analysis of total pre-rRNAs with probe ITS2 showed restoration of a normal pre-rRNA processing pattern.

**D)** RAMP quantification of the northern-blot shown in panel C. Product to precursor ratios in patient P3 LCLs at steps related to the processing of the large subunit rRNA precursors are expressed as variations relative to LCLs from the healthy control. Mean values  $\pm$  s.e.m. from three independent experiments.

**Figure 5. Variants in *HEATR3* impair 60S ribosomal subunit accumulation.**

**A)** Representative polysome profiles of lysates from LCLs derived from healthy individuals or patients (P2 and P4). The 40S subunit, 60S subunit, and 80S monosome are labeled. The vertical arrow highlights the reduction of 60S subunits in the samples from individuals P2 and P4.

**B)** Representative polysome profiles of lysates from LCLs transduced with lentiviruses expressing *HEATR3* or *GFP* cDNA. At least three independent experiments were performed with each cell line (A and B).

**Figure 6. Erythroid cell proliferation and differentiation are impaired in individuals with *HEATR3* variants**

**A)** Bone marrow aspirates of P2 (left panels) and P5 (right panels) with May-Grünwald-Giemsa staining, demonstrating a paucity (arrows) or absence (P5) of erythroid precursors and hypolobulated megakaryocytes (lower panels).

**B)** Cell count of purified CD34<sup>+</sup> from the peripheral blood of P2 (orange line) and a healthy control (blue line) subject to the erythroid culture assay was performed (n=1 to minimize invasiveness). Shown are cell counts on days 5, 7, 10, and 12.

**C)** Flow cytometry analysis of differentiating erythroid cells from P2 and a healthy control at days 10 and 12. ProE, proerythroblasts; EB, early basophilic erythroblasts; LB, late basophilic erythroblasts; Poly, polychromatophilic erythroblasts; Ortho, acidophilic erythroblasts.

**D)** Quantification of (C).

**E)** Real-time PCR quantification of *HEATR3* transcript levels in CD34<sup>+</sup> cells infected with lentiviral constructs expressing shRNAs targeting *HEATR3* or a scrambled control (SCR).

**F)** Cell numbers on days 5, 7, 10, and 12 of an erythroid culture assay after infection with the lentiviral vectors expressing *HEATR3* shRNAs.

**G)** Western blot analysis of the cells on day 7. Blots were probed with antibodies against HEATR3, p21, eS19 (RPS19), HSP70, GATA1, and pro-caspase 3. GAPDH was used as loading control.

**Figure 7. HEATR3 loss does not affect levels of p53, uL5, or uL18.**

**A)** Western blots of LCLs exposed to either 100 nM camptothecin (CPT) for 4 hours, or 10  $\mu$ M MG-132 for 6 hours, or the vehicle control, DMSO. Blots shown are probed with antibodies against p53. HEATR3 variants do not lead to p53 stabilization on their own, but they do, as expected, in combination with CPT or MG-132 treatments.

**B)** Quantification of (A) from three independent experimental replicates. Results shown are the relative levels of p53/actin.

**C)** Western blots of LCLs exposed to 100 nM CPT for 4 hours, or the vehicle control, DMSO. Blots shown are probed with antibodies against HEATR3, p53, uL5, and uL18.

**D)** Quantification of (C) from three independent experimental replicates. Results shown are the relative levels of uL5/actin or uL18/actin.

Figure 1

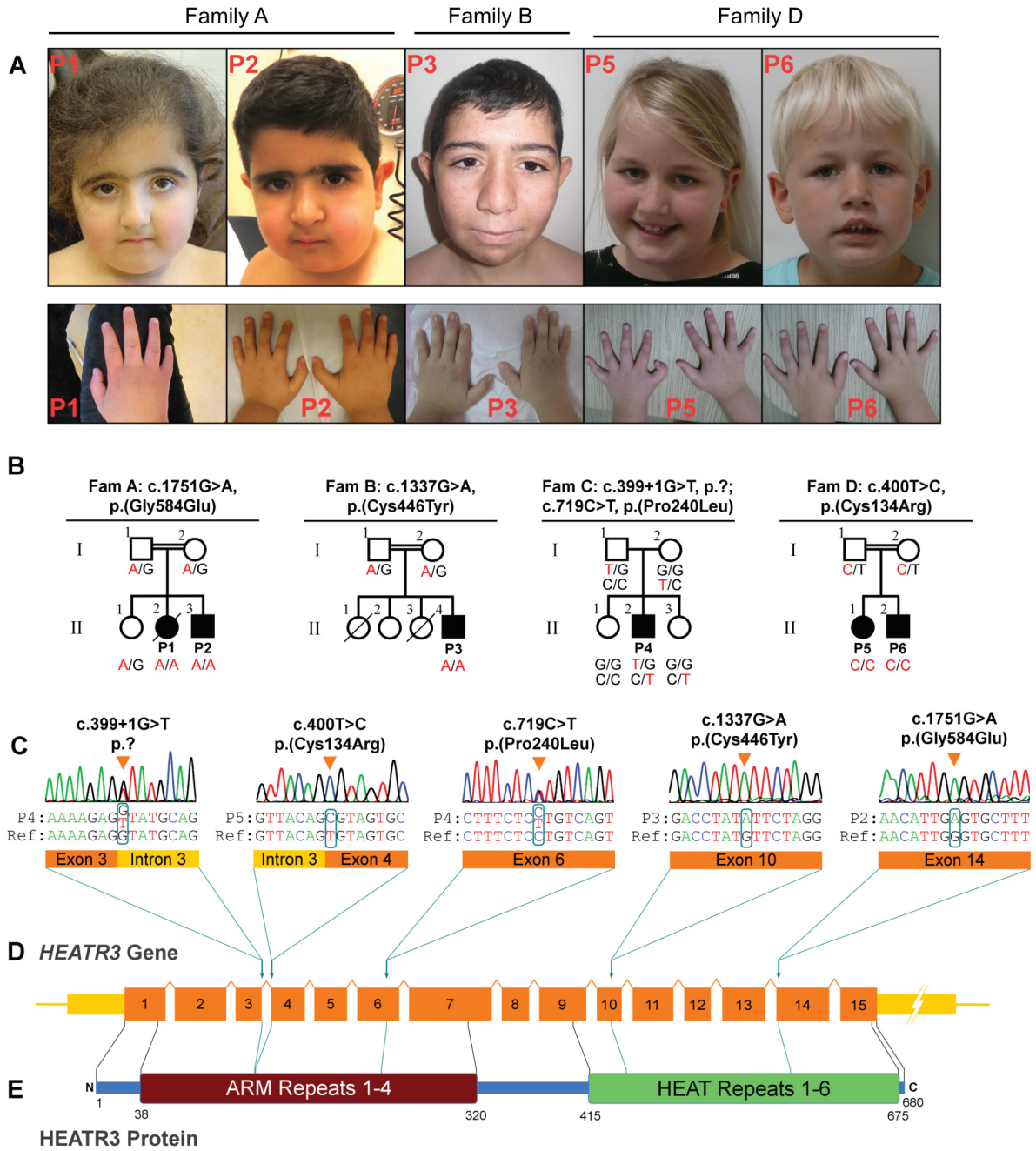


Figure 2

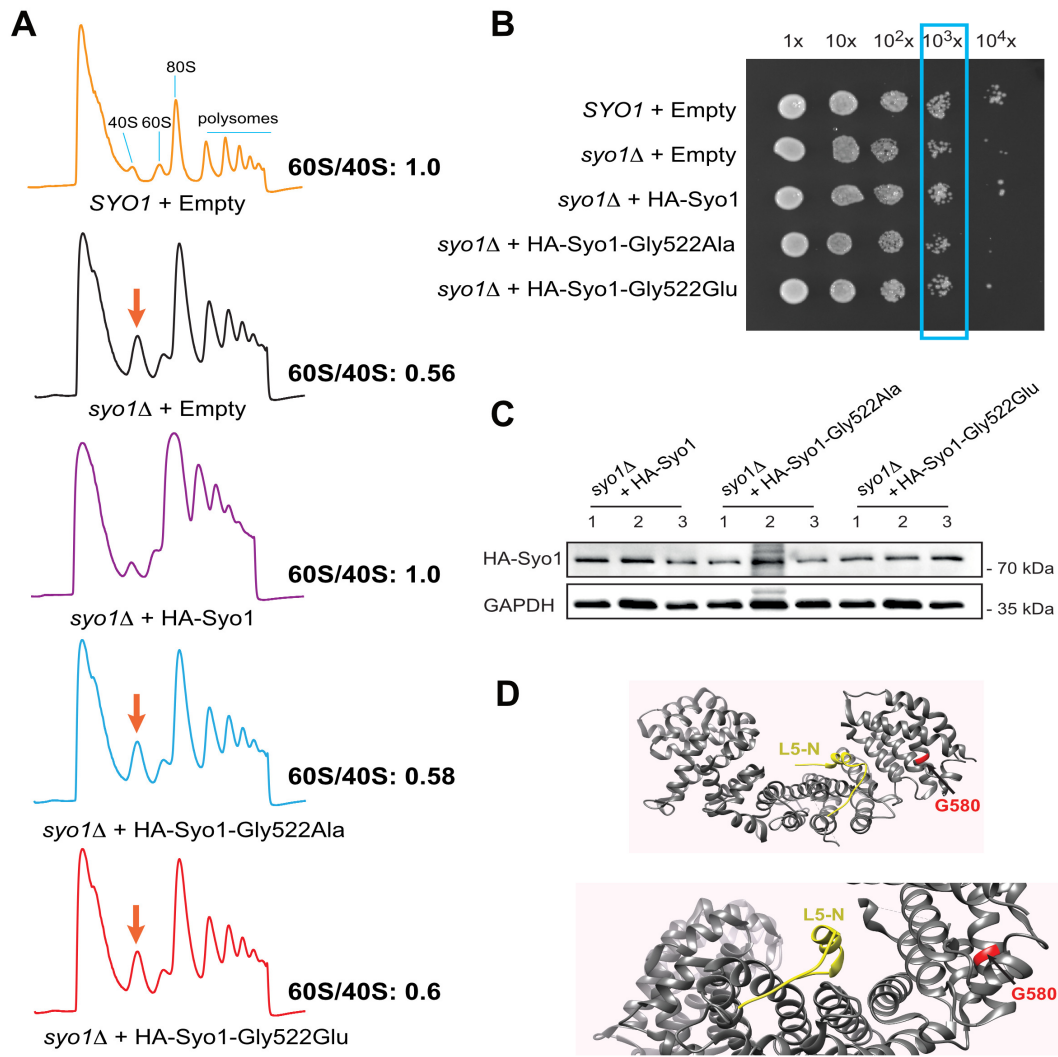
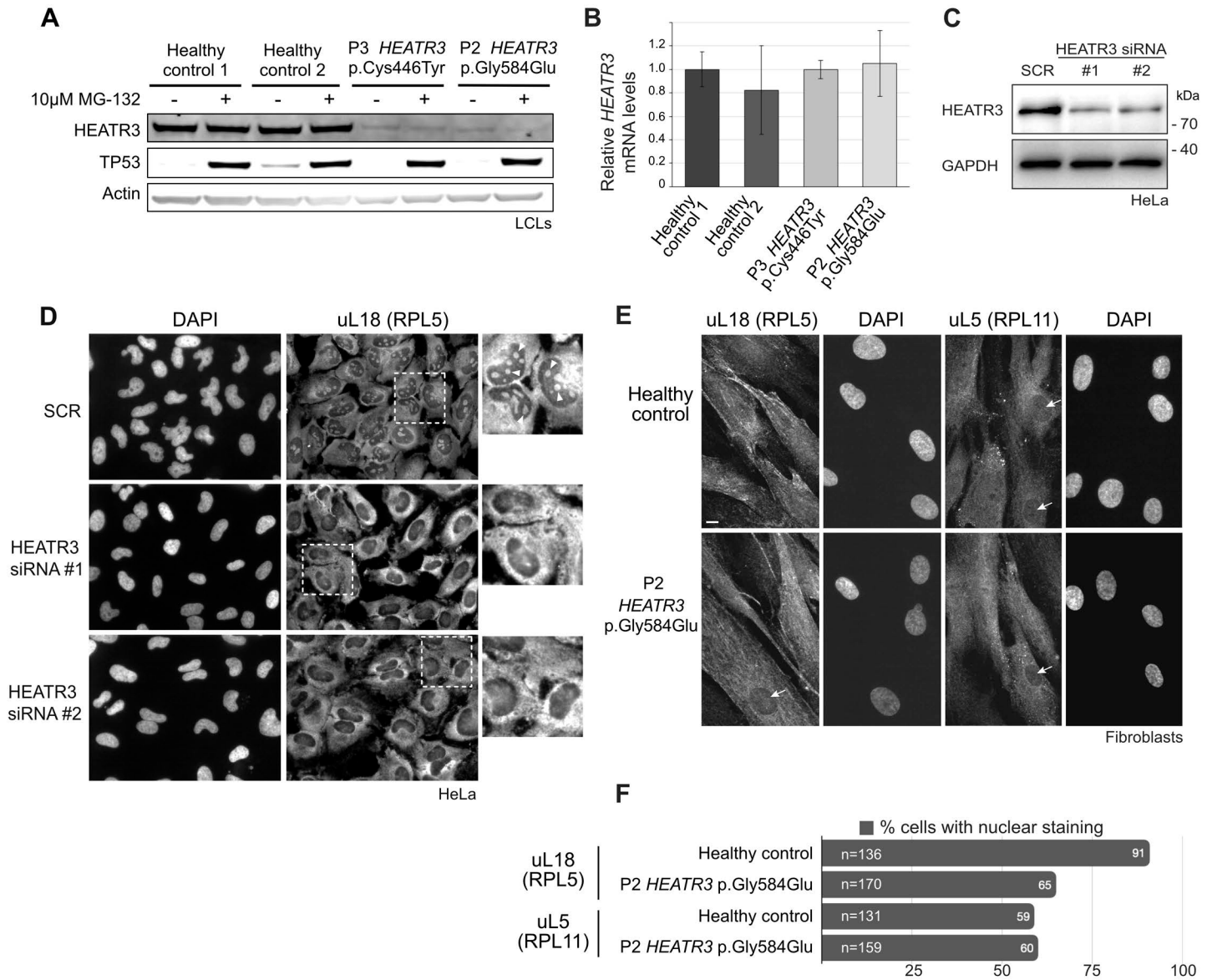


Figure 3



**Figure 4**

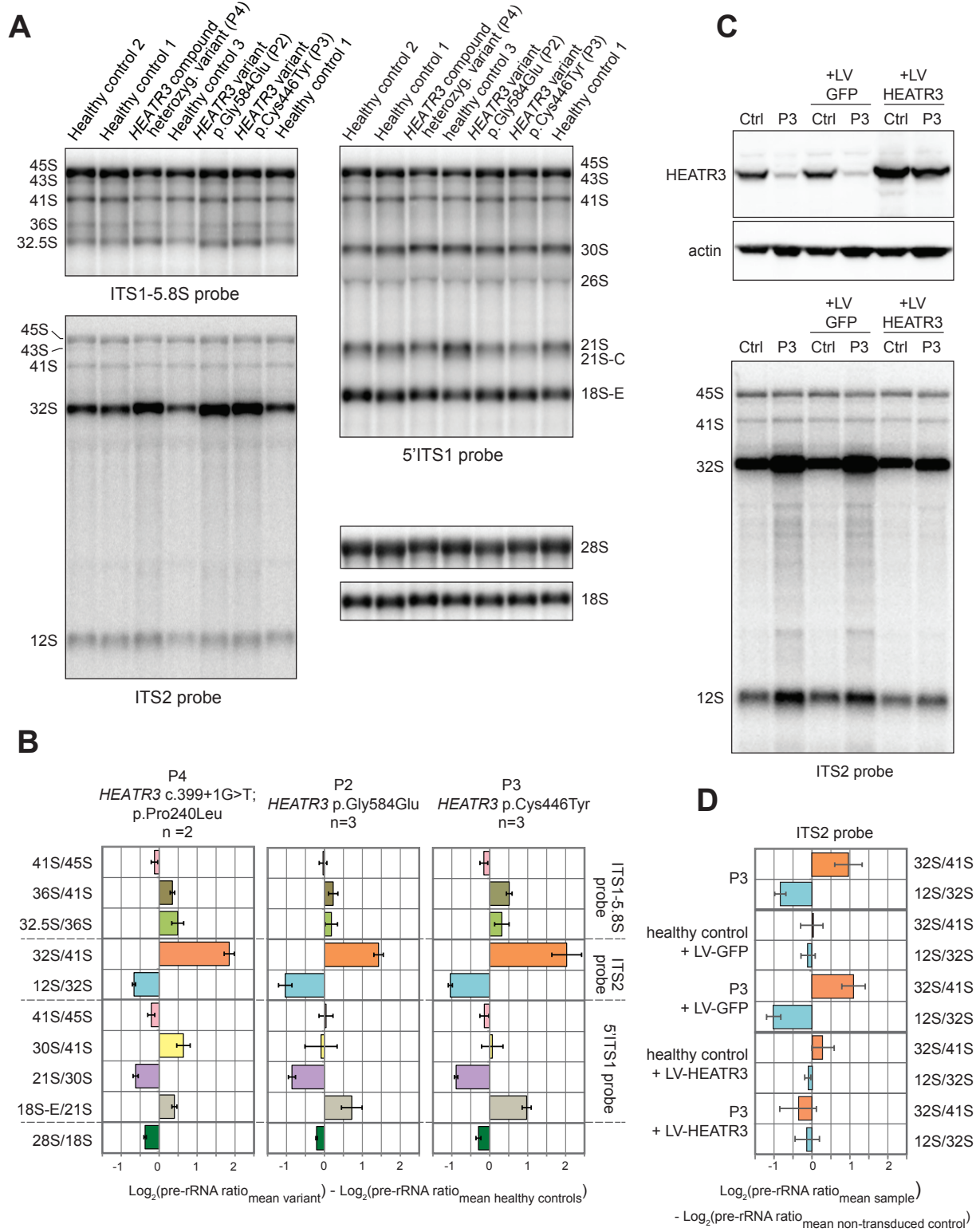


FIGURE 5

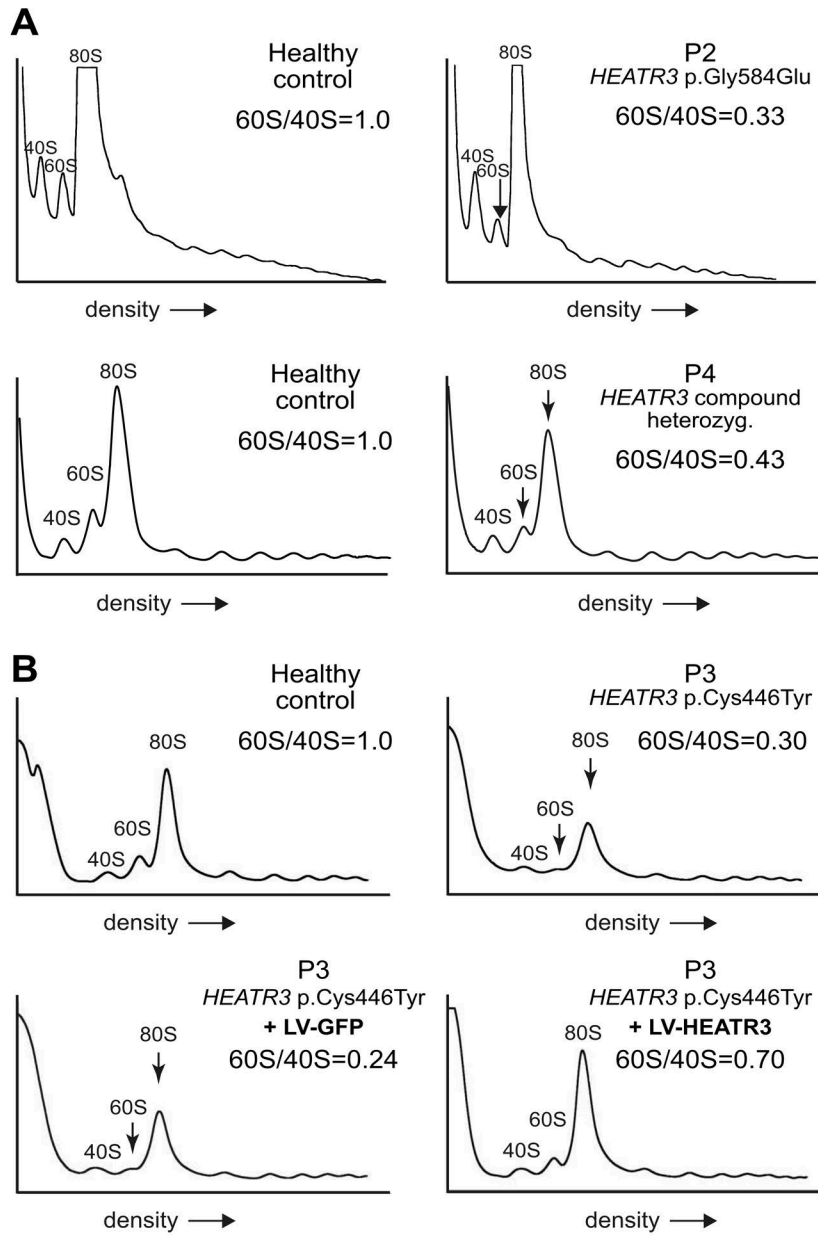


Figure 6

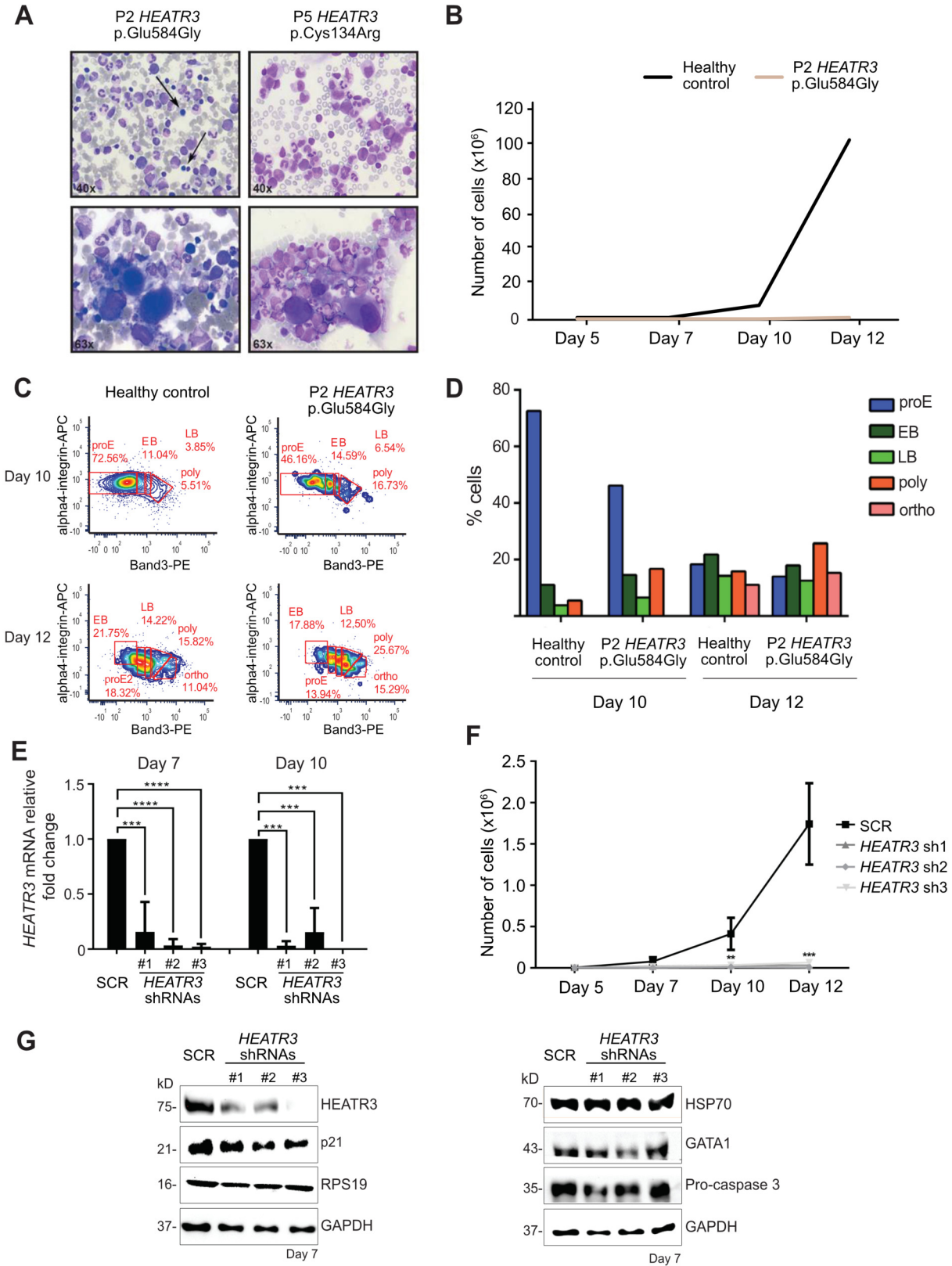


Figure 7

